Relationships between density and Young's modulus with microporosity and physico-chemical properties of Wistar rat cortical bone from growth to senescence

M. Vanleene, Christian Rey, Marie-Christine Ho Ba Tho

Relationships between density and Young's modulus with microporosity and physico-chemical properties of Wistar rat cortical bone from growth to senescence

M. Vanleene [a], C. Rey [b], M.-C. Ho Ba Tho [a,*]

[a] *Laboratoire de Biomécanique et génie Biomédical, CNRS-UMR 6600, Centre de Recherche de Royallieu, Université de Technologie de Compiègne, BP 20529, Compiègne cedex, France*

[b] *Centre Inter-Universitaire de Recherche et d'Ingénierie des Matériaux, CNRS-UMR 5085, ENSIACET-INPT, 118 rue de Narbonne, 31077 Toulouse cedex 4, France*

Abstract

The aim of this study is to assess density and elastic properties of Wistar rat cortical bone from growth to senescence and to correlate them with morphological and physico-chemical properties of bone. During growth (from 1 to 9 months), bone density and Young's modulus were found to increase from 1659 ± 85 to $2083 \pm 13\,\mathrm{kg\,m^{-3}}$ and from 8 ± 0.8 to 19.6 ± 0.7 GPa respectively. Bone microporosity was found to decrease from $8.1 \pm 0.7\%$ to $3.3 \pm 0.7\%$. Physico-chemical investigations exhibited a mineralization of bone matrix and a maturation of apatite crystals, as protein content decreased from $21.4 \pm 0.2\%$ to $17.6 \pm 0.6\%$ and apatite crystal size and carbonate content increased (c-axis length: from 151 to 173 Å and CO_3W%: from $4.1 \pm 0.3\%$ to $6.1 \pm 0.2\%$). At adult age, all properties stabilized. During senescence, a slow decrease of mechanical properties was first observed (from 12 to 18 months, $\rho = 2089 \pm 14$ to $2042 \pm 30\,\mathrm{kg\,m^{-3}}$ and E_3=19.8 ±1.3 to 14.8 ± 1.5 GPa), followed by a stabilization. Physico-chemical properties stabilized while microporosity increased slightly (from 3.3% to 4%) but not significantly ($p > 0.05$). A multiple regression analysis showed that morphological and physico-chemical properties had significant effects on density regression model. Microporosity had a greater effect on Young's modulus regression model than physico-chemical properties. This study showed that bone structure, mineralization and apatite maturation should be considered to improve the understanding of bone mechanical behaviour.

Keywords: Density; Elastic properties; Microporosity; Physico-chemical properties; Growth; Senescence

1. Introduction

Characterization of the mechanical properties of bone is important for evaluation of bone pathologies and their therapeutic treatments. These properties have been widely studied during the last forty years on human and animal models. They were found to be correlated to bone porosity [1–6] and to bone mineral content (ashes content) [7,8,2,9,3–5,10]. Further physico-chemical investigations of bone mineral matrix were performed more recently using vibrational spectroscopy [11–19]. Collagen fibers orientation and organization was also found to influence bone mechanical properties [20–24]. Several aspects of bone's physico-chemistry such as the influence of collagen matrix-apatite crystal interactions on bone mechanical properties have not yet been clearly explained.

Rat models are commonly used to investigate bone structural, mechanical and physico-chemical variation due to diseases [25–28] or physical activities [29–33]. Ageing is also a natural process inducing variation of bone properties and is widely investigated in literature. Rat models are useful in such investigations due to availability of young specimens. During ageing, a decrease of bone mineral density and bone mineral content was observed in vertebral bone of Sprague Dawley rats [34] but no variation was observed in vertebra, tibia or femur bone of Fisher F344 rats [35]. However, Kohles

* Corresponding author. Tel.: +33 344234918; fax: +33 344204813
E-mail address: marie-christine.hobatho@utc.fr (M.-C. Ho Ba Tho).

doi:10.1016/j.medengphy.2007.12.010

et al. have observed an increase of both density and elastic properties of femur cortical bone of F344 rats during ageing [36]. During growth and senescence, investigations of femoral bone in Sprague Dawley rats have shown an increase of apatite crystallinity and carbonate content, an increase of BMD and cross section diameters. Stiffness was found to not change with age but fracture resistance decreased dramatically during senescence [37]. To our knowledge, this study was the only one to investigate the mechanical, morphological and physico-chemical properties of cortical bone at the organ level during growth and senescence.

Previous studies used a wide range of techniques, rat strain and age which make difficult the knowledge of age impact on bone mechanical properties. Consequently, to have a better understanding of this variation through ageing, it is necessary to perform additional measurements such as tissue microporosity and physico-chemical properties over a longer period of time (from very young to old specimens) and to quantify the correlation between elastic, morphologic and physico chemical properties. In our study, we choose the Wistar rat model as it was used to investigate the mechanical properties of muscles through ageing [38]. Few studies are focused on the interaction between bone and muscle. Consequently, our study will allow further comprehension of the variation of both simultaneously through ageing.

2. Methods

Ten male RJHan:WI Wistar rats of each age, 1, 4, 9, 12, 18 and 24 months (from very young to old) were purchased from an authorized stock breeder (Janvier Inc., France) and were euthanized in agreement with French law (Decree 2001-486, 6 June 2001). Both femurs were harvested and were cut transversely at the proximal and distal end of the diaphysis with a diamond saw (Microcut, BROT Technologies, France). Diaphyseal lengths were 9.1 ± 1, 15.7 ± 1.5, 17.7 ± 1.3, 16.2 ± 2.2, 20.3 ± 1.1 and 19 ± 0.5 mm for 1, 4, 9, 12, 18 and 24 months old rat groups respectively. Bone marrow was then cleaned from the diaphyses using saline solution. Right femurs were dedicated to mechanical and morphological characterization. Left samples, dedicated to physico-chemical characterization, were lyophilized and ground at liquid nitrogen temperature (Freezer-Mill 6700, SPEX Certiprep, UK).

2.1. Assessment of mechanical properties

Bone density (ρ) was measured using a balance (Sartorius CP64, Sartorius AG, Germany) and a precision density measurement kit (Mettler Toledo GmbH, Switzerland) based on the Archimedes' principle. Longitudinal elastic properties of diaphyses were assessed in wet condition using a ultrasonic transmission technique [39]. This technique used two longitudinal ultrasound transducers (E9941, Valpey Fisher Corp., MA, USA) at low frequency (100 kHz). A generator (Tektronix TM504, Tektronix UK Ltd., UK) sent impulsions received by the first transducer acting as a transmitter. Ultrasonic waves were propagated through the sample, received by the second transducers and were visualized on an oscilloscope (Tektronix TDS 3032, Tektronix UK Ltd., UK). The ultrasound velocity (V_{bar}) was calculated from the time of wave propagation and from the diaphyseal length, measured with an electronic micrometer (Digimatic Outside Micrometer, Mitutoyo, Japan). Ultrasound velocity could be used along with bone density to calculate the longitudinal Young's modulus (E_3) as length of ultrasound wave used (2 cm) was far more important that femur cross section diameters (from about 2 to 5 mm) [39,40]:

$$E_3 = \rho V_{bar}^2$$

Reproducibility for ρ and E_3 was assessed by performing tests three times for each sample.

2.2. Assessment of microporosity

Proximal femur cross section were ground with abrasive papers (P600, P800, P1200), polished on microcloths with successively finer grades of alumina powder (1, 0.3, 0.02 μm) and dried at room temperature. Complete images of proximal cross section of femurs were first reconstructed from about 10 partial images (pixel resolution: 2 μm) using an environmental scanning electron microscope (Philips XL30 ESEM-FEG, Royal Philips Electronics, the Netherlands). As no difference of microstructure was qualitatively observed, four images of the cortex from different random areas of the cross-section were obtained with a better resolution (field of view: 1 mm $\times$ 0.7 mm, pixel resolution: 0.717 μm).

Images were analysed using Q WinStandard image analysis software V2.7 (Leica Microsystems Imaging Solution Ltd., UK). Percentage of porosity (%poro) was calculated from the total pore area, including canals and lacunae, divided by the total cross sectional area. Reproducibility was assessed on one sample per group by repeating the complete analysis twice.

2.3. Assessment of physico-chemical properties

Three different methods were performed on left femur samples.

First, Fourier Transformed Infra Red (FTIR) spectroscopy analyses were performed on six samples per age group (1760-X FTIR Spectrometer, PerkinElmer Inc., MA, USA). The spectra were curve-fitted in the ν_4 PO_4, ν_2 CO_3 and collagen amide band domains (Galactic GRAMS software, NH, USA).

Several parameters were extracted from FTIR data corresponding to band intensity (band area) ratio of representative species relative to all ν_4 phosphate domain bands: PO_4 species in apatite lattice (sum of 600, 575 and 560 cm^{-1} bands), non-apatitic HPO_4 ions located in a hydrated layer on apatite crystal surface (534 cm^{-1} band), type A CO_3, type B CO_3 species in apatite lattice (879

and 871 cm^{-1} bands), non apatitic CO_3 species (866 cm^{-1} band) and collagen amide I species (1650 cm^{-1} band) [11,41,12].

Second, two chemical analyses were performed on samples. Carbonate weight percentage (CO_3W%) was measured on six samples per age group using a CO_2 Coulometer (Coulometrics Inc., Co, USA). Protein nitrogen weight content was analysed on three samples per age group using a Elemental Analyser EA 1110 CHNS (Thermo Fisher Scientific Inc., MA, USA). Elemental analysis precision is 0.3%. Protein weight percentage of bone (PW%) was then obtained from nitrogen content in collagen [42].

Third, as previous analyses consumed most of sample powder, specimens were pooled in each age group. X-ray diffraction was recorded with a X-ray diffractometer (Inel CPS 120, Enraf Nonius SA, France) using Co radiation (X-ray wavelength = 1789 Å). Two peaks at 30° and 45° (2θ) were identified respectively to 002 (c-axis of apatite lattice) and 310 diffraction planes of the apatite crystals. By measuring the width of these diffraction peaks and applying the Scherrer formula, it was possible to calculate the average dimensions of the diffraction domains and thus, apatite crystal apparent length and width [43].

2.4. Statistical analysis

Statistical analyses were performed using the software Statgraphics Plus Version 5.0 (Statistical Graphics Corp., USA). Comparison of variables was undertaken using non parametric Mann and Whitney tests ($p < 0.05$). In order to correlate mechanical properties with morphological and physico-chemical properties, multiple regression analyses were performed with data from 1 to 24 months old rats. Data were normalized between 0 and 1 using maximum and minimum values as landmark in order to assess the respective strength of each variable in the explanatory regression model. To check relevance of each variable in the regression model, their respective coefficients were compared to the zero value.

3. Results

3.1. Mechanical properties

Reproducibility for density and Young's modulus values varied from 0.1% to 1% and from 2% to 6% respectively according to different age group. These range were lower than that of variations within the group: 1–5% and 6–10% respectively. Values for 1, 4, 9, 12, 18, 24 months specimens were respectively 1659 ± 85, 1991 ± 27, 2083 ± 13, 2089 ± 14, 2042 ± 30, 2031 ± 25 kg m^{-3} for density and 8 ± 0.8, 17.2 ± 1, 19.6 ± 0.7, 19.8 ± 1.3, 17.8 ± 1.5, 14 ± 0.9 GPa for Young's modulus. ρ and E_3 were found to increase significantly ($p < 0.05$) between 1 month and 4 months groups: +20.1% and +114.6% respectively. A significant increase was also observed between 4 and 9 months groups ($p < 0.05$): +4.6% for ρ and +13.8% for E_3. A stabilization was then observed between 9 and 12 months groups ($p > 0.05$) and followed by a significant decrease between 12 and 18 months groups ($p < 0.05$): −2.3% and −25.1% respectively. No significant variation was found between 18 and 24 months groups ($p > 0.05$). ρ and E_3 values were illustrated in Figs. 1 and 2.

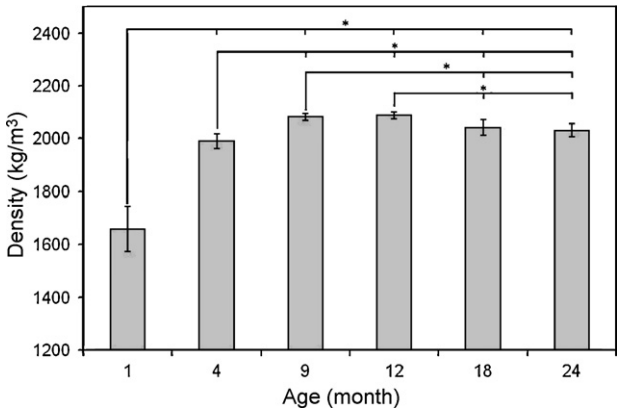

Fig. 1. Variation of cortical bone density of Wistar rat during growth and senescence (mean and standard variation, ∗statistically significant difference, $p < 0.05$).

3.2. Microporosity

Tissue morphology of femur cross section evolved during growth from a porous structure (1 month) to a lamellar structure for periosteum and a porous structure for endosteum (4 and 9 months). For mature specimens (9 and 12 months), bone morphology seemed constant with both lamellar and porous structures. During senescence (18 and 24 months), some specimens exhibited larges pores in the endosteum. Pores were not related to the Haversian structure as no concentric lamellae were observed around the pores. Fig. 3

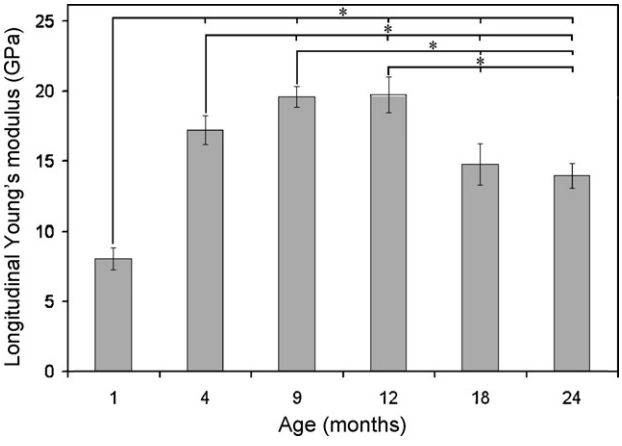

Fig. 2. Variation of Young's modulus of Wistar rat cortical bone in the longitudinal direction during growth and senescence (mean and standard variation, ∗statistically significant difference, $p < 0.05$).

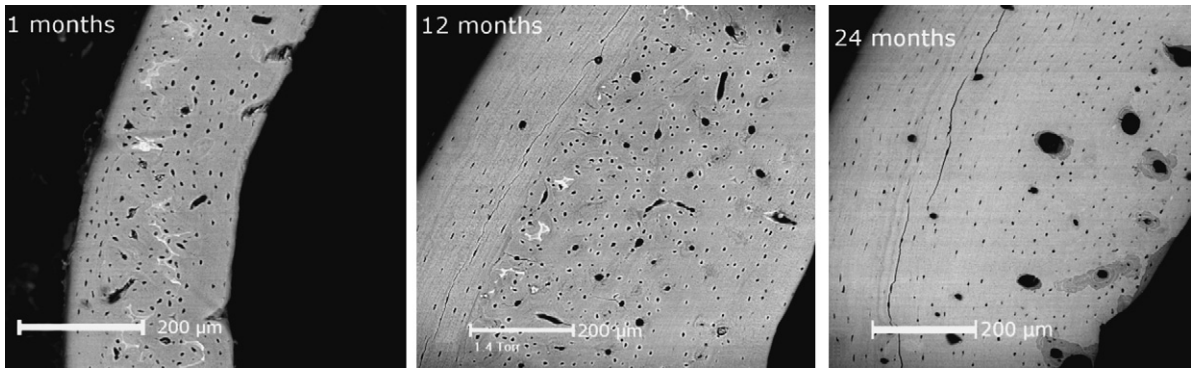

Fig. 3. ESEM images of femur proximal cross-section of 1, 12 and 24 months old specimens of Wistar rat.

illustrates femur cross section morphology for young, mature and old Wistar rats. Microporosity values for 1, 4, 9, 12, 18 and 24 months old specimens were respectively $8.1 \pm 0.7\%$, $3.2 \pm 0.5\%$, $3.3 \pm 0.7\%$, $2.5 \pm 0.6\%$, $3.2 \pm 0.9\%$ and $4 \pm 1.5\%$. Reproducibility varied from 2% to 5.6% of the value according to the different age groups. Bone microporosity was found to decrease significantly between 1 month and 4 months groups ($p < 0.05$). No significant variation was found between 4, 9 and 12 months groups ($p > 0.05$). Microporosity increased between 12, 18 and 24 months groups but variations were not statistically significant ($p > 0.05$). Microporosity data are illustrated in Fig. 4.

3.3. Physico-chemical properties

FTIR investigations of bone matrix exhibited no statistically significant difference between groups for apatitic PO_4band and non-apatitic HPO_4 band intensity ratio during growth and senescence ($p > 0.05$). However, a tendancy to increase for apatitic phosphate and to decrease for labile phosphate were observed. Analysis of type A, type B CO_3 and labile CO_3 band intensity ratio showed no significant difference between the 1 and 4 months groups ($p > 0.05$).

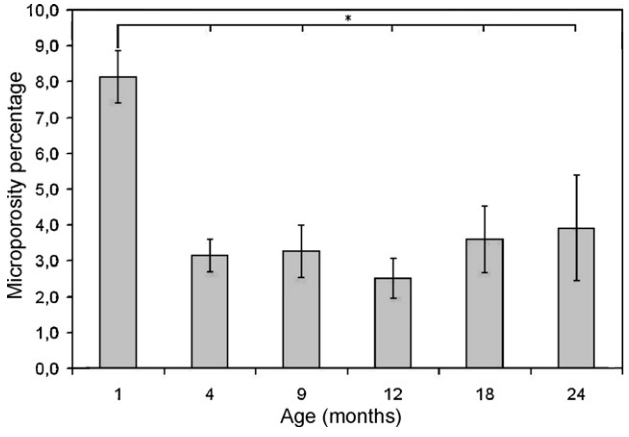

Fig. 4. Variation of femur cross-sectional porosity percentage during growth and senescence (mean and standard variation, ∗statistically significant difference, $p < 0.05$).

Table 1
FTIR band intensity ratio of apatitic phosphate, labile phosphate and amide I on total phosphate (mean and standard deviation)

Specimen age	Apatite PO_4/PO_4	Labile HPO_4/PO_4	Amide I/PO_4
1 month	0.69 ± 0.05	0.23 ± 0.03	0.87 ± 0.77
4 months	0.69 ± 0.02	0.22 ± 0.02	0.78 ± 0.03
9 months	0.70 ± 0.05	0.21 ± 0.04	0.77 ± 0.02
12 months	0.73 ± 0.03	0.19 ± 0.02	0.74 ± 0.02
18 months	0.71 ± 0.05	0.22 ± 0.03	0.78 ± 0.1
24 months	0.71 ± 0.05	0.19 ± 0.02	0.75 ± 0.05

Table 2
FTIR band intensity ratio of type A, type B and labile carbonate on total phosphate (mean and standard deviation)

Specimen age	Type A CO_3/PO_4	Type B CO_3/PO_4	Labile CO_3/PO_4
1 month	0.0092 ± 0.012	0.0192 ± 0.0025	0.0336 ± 0.0061
4 months	0.0094 ± 0.0006	0.0199 ± 0.0008	0.0379 ± 0.0034
9 months	0.0109 ± 0.0007	0.0228 ± 0.0009	0.0466 ± 0.0035
12 months	0.0109 ± 0.0003	0.0228 ± 0.0003	0.0427 ± 0.0029
18 months	0.0103 ± 0.0008	0.0221 ± 0.0016	0.0436 ± 0.0063
24 months	0.0111 ± 0.0007	0.0234 ± 0.0008	0.047 ± 0.0044

A statistically significant increase of band intensity ratio was observed between the 4 and 9 months groups ($p < 0.05$), then a stabilization was observed between the 9, 12, 18, 24 months groups ($p > 0.05$). Amide I band intensity ratio values were found to decrease significantly between 1 month and 4 months ($p < 0.05$). No significant variation was found between the 4 and 9 months groups ($p > 0.05$). Values were found to decrease significantly between the 9 and 12 months groups ($p < 0.05$) and to stabilize between the 12, 18 and 24 months groups ($p > 0.05$). Band intensity ratio of phosphate, carbonate and amide I are reported in Tables 1 and 2.

CO_3W% and PW% variations observed on chemical analyses confirmed variations observed on FTIR analyses. Values for 1, 4, 9, 12, 18, 24 months old groups were respectively 4.1 ± 0.3, 4.9 ± 0.2, 6.1 ± 0.2, 6.1 ± 0.2, 6.0 ± 0.2, $6.0 \pm 0.2\%$ for CO_3W% and 21.4 ± 0.2, 19 ± 0.7, 17.6 ± 0.6, 18.3 ± 0.8, 17.8 ± 0.6, $17.4 \pm 0.2\%$ for PW%. A statistically significant increase of CO_3W% and decrease of PW% were observed between 1, 4, 9 months groups ($p < 0.05$). Then, stabilizations of CO_3W% and PW% were observed

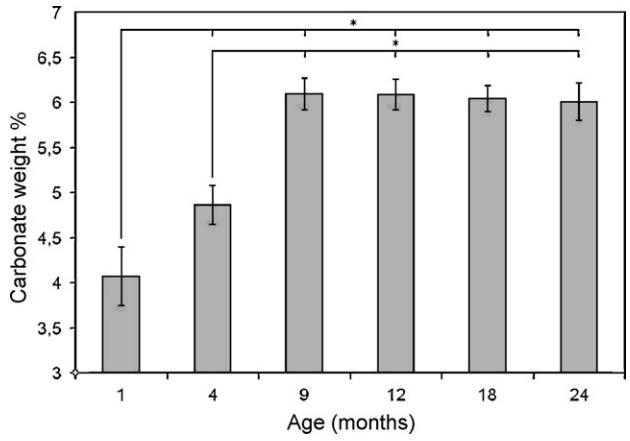

Fig. 5. Variation of carbonate weight content of bone matrix during growth and senescence (mean and standard variation, ∗statistically significant difference, $p < 0.05$).

between 9, 12, 18 and 24 months groups ($p > 0.05$). $CO_3W\%$ and PW% data are illustrated in Figs. 5 and 6 respectively.

X-ray diffraction assessments showed a slow increase of the width of diffraction peaks attributed to 002 and 310 lattice planes of apatite crystals. This led to an increase of apparent crystal dimensions: 151, 169, 173, 186, 178 and 199 Å for crystal length and 61, 65, 76, 70, 65, 72 Å for crystal width for 1, 4, 9, 12, 18, 24 months old group respectively.

3.4. Correlation of bone properties

Multiple regression analysis performed on normalized data from 1 to 24 months groups gave the following relationships between density and Young's modulus with morphological and physico-chemical properties:

$$\rho = 0.79 - 0.46 \times \%\text{poro} + 0.27 \times CO_3W\% - 0.18 \times PW\%, \quad r^2 = 0.889$$

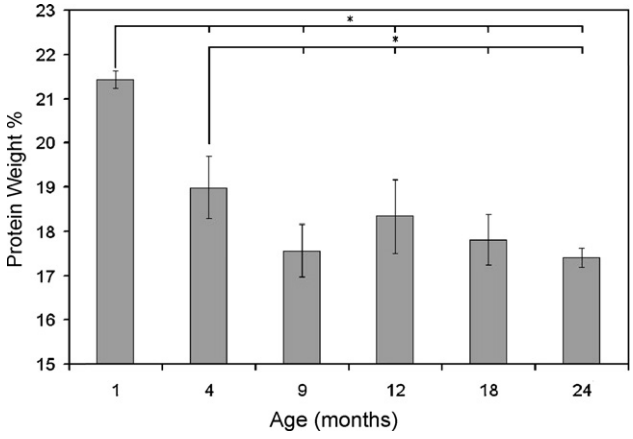

Fig. 6. Variation of protein weight content of bone matrix during growth and senescence (mean and standard variation, ∗statistically significant difference, $p < 0.05$).

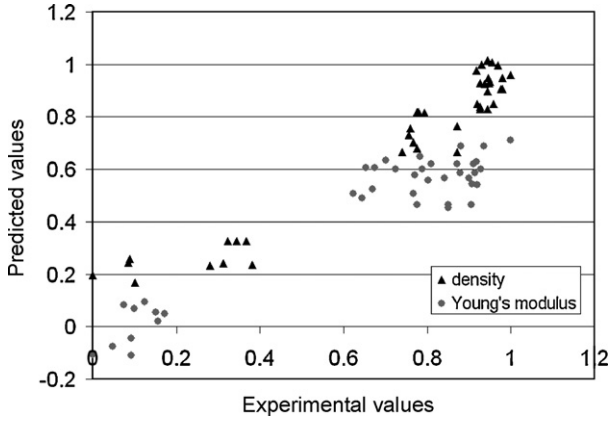

Fig. 7. Scatterplot of data from correlation models versus experimental data of cortical bone density and Young's modulus of Wistar rat.

$$E_3 = 0.71 - 0.82 \times \%\text{poro} + 0.17 \times CO_3W\% + 0.11 \times PW\%, \quad r^2 = 0.738$$

In the regression model of density variation, all variable coefficients were significantly different from 0 ($p < 0.05$). This regression analysis showed that density variation was correlated to morphological and physico-chemical parameters. In the regression model of Young's modulus variation, only %poro coefficient was significantly different from 0 ($p < 0.05$). Correlation model relevance is illustrated in a scatterplot of standardized data in Fig. 7.

4. Discussion

4.1. Mechanical properties

One study found similar Young's modulus and density except for variation through senescence [36]. Besides, variation of mechanical properties differed at the senescence. This may be related to the different rat strain used. The range of BMD values (1244–1398 mg mm^{-3}) found by Banu et al. on femoral diaphysis of F344 rats was lower than our study, most likely because techniques used were different. However, they found similar variation through ageing [35]. Moreover, in comparison with human data, similar values of ρ and E_3 were observed at the adult age: $\rho_{human} = 1821 \pm 183$ kg m^{-3} and $E_{3human} = 19.9 \pm 2.7$ GPa [44] but variation through senescence is different. These previous comparisons showed discrepancies demonstrating the need of additional investigations (morphological and physico-chemical) at different scales to understand the variation of mechanical properties in bone during ageing.

4.2. Microporosity

The observed variation of bone microporosity resulted from variations of bone tissue architecture (Fig. 4). Thus, dur-

ing growth, a decrease of microporosity was related to active apposition of a periosteal lamellar bone which exhibited a low porosity [45]. During senescence, global microporosity increased and large pores could be observed in the endosteum, which could be related to a resorption phenomenon [45].

To our knowledge, such variation of microporosity has not previously been demonstrated as equivalent data are not available. Akkus et al. [37] observed cross section diameter variation but did not investigate bone microporosity. Wistar rat exhibited lower values than adult human bone in which porosity values vary from 10% to 40% [46,40]. Variation of bone porosity during senescence differed also as human bone porosity showed a significant increase.

4.3. Physico-chemical properties

Physico-chemical variations observed from 1 to 9 months seemed to be consistent with that reported for other vertebrates [37,47,13,48]. Increase of total carbonate content with age, especially in young animals, seemed associated with a slight decrease of non apatitic HPO_4^{2-}band intensity ratio and appeared as a constant feature during animal growth [12,13,49]. This phenomenon was also observed during ageing of synthetic apatitic precipitates [13] and has been associated with the maturation of the mineral latice. During this process, there is no significant change in the distribution of the different carbonate species and of the apatite stoichiometry. At any stage, OH^- species could not be detected by FTIR as it is usually the case in bone [11,14]. The increase of the labile carbonate band intensity ratio assessed during the growth period was not in agreement with the decrease reported in previous literature [12,13] and could be explained by the intensive apposition of new bone rich of labile carbonate on the perisoteal surface. The increase in crystal dimensions in rats has been also observed in synthetic apatitic preparations during crystal maturation, and seemed associated with an increase of the apparent size of apatitic domains although the application of Scherrer formula neglected the effect of crystal imperfections on XRD bands broadening. Globally, the increase in crystal perfection has also be observed in FTIR or Raman spectra of bone tissue characterized by thinner mineral bands during growth and ageing [37]. Analyses demonstrated also a mineralization of bone matrix with a decrease of the protein content during growth. In the present study, we did not report information on the collagen matrix, especially the cross links, due to uncertainties in bands assignment [50].

Physico-chemical analyses during senescence (from 12 to 24 months) enlightened a stabilization of FTIR band intensity ratio and all chemical parameters of bone were found to be constant (PW%, CO_3W%). This could be interpreted as equilibrium between bone apposition and resorption at the femur surface. During bone maturation, our physico-chemical results were in agreement with analyses performed by Akkus et al. [37] but our results differed for senescence as they found a continuous mineralization. This difference may be due to the difference of rat strains.

4.4. Multiple regression analyses

The regression models showed that microporosity has a negative effect on both density and Young's modulus. Maturation and mineralization of bone matrix has a positive effect on density, with an increase in mineralization and maturation increasing the density of bone matrix. However, effects of bone matrix composition were found not to be statistically relevant for the Young's modulus model. These results demonstrated that density is a parameter more relevant than elasticity when it comes to investigate alterations of the bone matrix composition.

5. Conclusion

In the present study, correlation of mechanical properties with morphological and physico-chemical properties was investigated from growth to senescence. Young's modulus regression model indicated a greater relationship with microporosity variation than that of bone matrix composition. On the contrary, bone density regression model was found to be dependent on both microporosity and physico-chemical properties.

The increase of mechanical properties during growth was related to a decrease of microporosity and increase of bone matrix maturation. These results are different for human during growth as no decrease of porosity is expected and bone matrix maturation is likely to occur. During senescence, decrease of mechanical properties seemed to be more related to increase of microporosity as no change in physico-chemical properties was observed. Such porosity increase is also observed for human during senescence but at a larger scale. Furthermore, our qualitative data suggested that this difference may be related to the difference of tissue microstructure.

To conclude, our study showed that combined investigations of microstructural and physico-chemical properties of bone tissue are of importance to have a better understanding of the variation of bone mechanical behaviour.

Acknowledgments

This study was supported by the French national scientific research center "Centre National de la Recherche Scientifique" (CNRS) and the French national institute of Health "Institut National de la Santé Et de la Recherche Médicale" (INSERM) through a joint program IT2B "Ingénierie Tissulaire Biomécanique et Biomatériaux". The authors would like also to acknowledge the reading and advices of Dr Sandra Shefelbine.

Conflict of interest statement

The authors certify that the present study was not influenced by other private or professional interests.

References

[1] Katz J, Yoon H, Lipson S, Maharidge R, Meunier A, Christel P. The effect of remodeling on the elastic properties of bone. Calcif Tissue Int 1984;36:31–S36.

[2] Currey J. The effect of porosity and mineral content on the Young's modulus of elasticity of compact bone. J Biomech 1988;21(2):131–9.

[3] Schaffler M, Burr D. Stiffness of compact bone: Effects of porosity and density. J Biomech 1988;21(1):13–6.

[4] Martin RB, Ishida J. The relative effects of collagen fiber orientation, porosity, density, and mineralization on bone strength. J Biomech 1989;22(5):419–26.

[5] McCalden R, McGeough J, Barker M, Court-Brown C. Age-related changes in the tensile properties of cortical bone. J Bone Joint Surg 1993;75-A(8):1193–205.

[6] Bensamoun S, Gherbezza JM, De Belleval JF, Ho Ba Tho MC. Transmission scanning acoustic imaging of human cortical bone and relation with the microstructure. Clin Biomech 2004;19:639–47.

[7] Currey J. Changes in the impact energy absorption of bone with age. J Biomech 1979;12(6):459–69.

[8] Currey J. Effects of differences in mineralization on the mechanical properties of bone. Phil Trans R Soc Lond B 1984;304:509–18.

[9] Currey J, Brear K, Zioupos P. The effect of ageing and changes in mineral content in degrading toughness of human femora. J Biomech 1996;29(2):257–60.

[10] Yeni Y, Brown C, Norman T. Influence of bone composition and apparent density on fracture toughness of the human femur and tibia. Bone 1998;22(1):79–84.

[11] Rey C, Lian J, Grynpas M, Shapiro F, Zylberberg L, Glimcher M. Non-apatitic environment in bone mineral: Ft-ir detection, biological properties and changes in several disease states. Connect Tissue Res 1989;21:267–73.

[12] Rey C, Renugopalakrishnan V, Collins B, Glimcher M. Fourier transformed infrared spectroscopy study of the co_3 ions in the bone mineral during ageing. Calcif Tissue Int 1991;49:251–8.

[13] Rey C, Hina A, Tofighi A, Glimcher M. Maturation of poorly crystalline apatites: Chemical and structural aspects in vivo and in vitro. Cells Mater 1995;5(4):345–56.

[14] Rey C, Miquel J-L, Facchini L, Legrand A, Glimcher M-J. Hydroxyl groups in bone mineral. Bone 1995;16:583–6.

[15] Boskey A. Mineral-matrix interactions in bone and cartilage. Clin Orthop Relat Res 1992;281:244–74.

[16] Boskey A, Mendelsohn R. Infrared spectroscopic characterization of mineralized tissues. Vib Spectrosc 2005;38(1-2):107–14.

[17] Boskey A. Assessment of bone mineral and matrix using backscatter electron imaging and ftir imaging. Curr Osteopor Rep 2006;4(2):71–5.

[18] Paschalis E, DiCarlo E, Betts F, Sherman P, Mendelshon R, Boskey A. Ftir microspectroscopic analysis of human osteonal bone. Calcif Tissue Int 1996;59:480–7.

[19] Paschalis E, Betts F, DiCarlo E, Mendelshon R, Boskey A. Ftir microscpectroscopic analysis of normal human cortical and trabecular bone. Calcif Tissue Int 1997;61:480–6.

[20] Lee S, Davidson C. The role of collagen in the elastic properties of calcified tissue. J Biomech 1977;10:473–86.

[21] Mehta S, Öz O, Antich P. Bone elasticity and ultrasound velocity are affected by sublte changes in the organic matrix. J Bone Miner Res 1998;13(1):114–21.

[22] Zioupos P. Ageing human bone: Factors affecting its biomechanical properties and the role of collagen. J Biomater Appl 2001;15:187–229.

[23] Carden A, Rajachar R, Morris M, Kohn D. Ultrastructural changes accompagnying the mechanical deformation of bone tissue: a Raman imaging study. Calcif Tissue Int 2003;72:166–75.

[24] Morris M, Finney W, Rajachar R, Kohn D. Bone tissue ultrastructural response to elastic deformation probed by Raman spectroscopy. Faraday Discuss 2004;126:159–68.

[25] Peng Z-Q, Väänänen HK, Zhang HX, Tuukkanen J. Long-term effect of ovariectomy on the mechanical properties and chemical composition of rat bone. Bone 1997;20(3):207–12.

[26] Han SM, Szarzanowicz TE, Ziv I. Effect of ovariectomy and calcium deficiency on the ultrasound velocity, mineral density and strength in the rat femur. Clin Biomech 1998;13:480–4.

[27] Tuukkanen J, Koivukangas A, Jämsä T, Sundquist K, Mackay C, Marks Jr S. Mineral density and bone strength are dissociated in long bones of rat osteopetrotic mutations. J Bone Miner Res 2000;15(10):1905–11.

[28] Jämsä T, Rho JY, Fan Z, MacKay CA, Marks SC. Mechanical properties in long bones of rat osteopetrotic mutations. J Biomechan 2002;35:161–5.

[29] Umemura Y, Ishiko T, Yamauchi T, Kurono M, Mashiko S. Five jumps per day increase bone mass and breaking force in rats. J Bone Miner Res 1997;12(9):1480–5.

[30] Mosley JR, March BM, Lynch J, Lanyon LE. Strain magnitude related changes in whole bone architecture in growing rats. Bone 1997;20(3):191–8.

[31] Indrekvam K, Schnell Husby O, Gjerdet NR, Engester LB. Age-dependent mechanical properties of rat femur. Acta Orthop Scand 1991;62(3):248–52.

[32] Kohles SS, Bowers JR, Vailas AC, Vanderby R. Effect of hypergravity environment on cortical bone elasticity in rats. Calcif Tissue Int 1996;59:214–7.

[33] Kannus P, Jarvinen TL, Sievanen H, Kvist M, Rauhaniemi J, Maunu VM, et al. Effects of immobilization, three forms of remobilization, and subsquent deconditioning on bone mineral content and density in rat femora. J Bone Miner Res 1996;11(9):1339–46.

[34] Wang L, Banu J, McMahan C, Kalu D. Male rodent model of age related bone loss in men. Bone 2001;29(2):141–8.

[35] Banu J, Wang L, Kalu DN. Age-related changes in bone mineral content and density in intact male F344 rats. Bone 2002;30(1):125–30.

[36] Kohles SS, Cartee GD, Vanderby R. Cortical elasticity in aging rats with and without growth hormone treatments. J Med Eng Technol 1996;20(4-5):157–63.

[37] Akkus O, Adar F, Schaffler MB. Age-related changes in physicochemical properties of mineral crystals are related to impaired mechanical function of cortical bone. Bone 2004;34:443–53.

[38] Bensamoun S, Stevens L, Fleury M-J, Bellon G, Goubel F, Ho Ba Tho M-C. Macroscopic-microscopic characterization of the passive mechanical properties in rat soleus muscle. J Biomechan 2006;39(3):568–78.

[39] Ashman RB, Cowin SC, Van Buskirk WC, Rice JC. A continuous wave technique for the measurement of the elastic properties of cortical bone. J Biomechan 1984;17(5):349–61.

[40] Bensamoun S, Ho Ba Tho MC, Luu S, Gherbezza JM, De Belleval JF. Spatial distribution of acoustic and elastic properties of human femur cortical bone. J Biomechan 2004;37(4):503–10.

[41] Rey C, Shimizu M, Collins B, Glimcher M. Resolution-enhanced fourier transform infrared spectroscopy study of the environment of phosphate ions in the early deposits of a solid phase of calcium-phosphate in bone and enamel, and their evolution with age. investigation in the ν_4 PO_4 domain. Calcif Tissue Int 1990;46:384–94.

[42] Glimcher M, Krane S. The organization and structure of bone and the mechanism of calcification. Academic Press; 1968.

[43] Grynpas M, Tenenbaum H, Holmyard D. The merge and maturation of the first apatite crystal in an in vivo bone formation. Connect Tissue Res 1989;21:227–37.

[44] Ho Ba Tho MC, Rho JY, Ashman RB. Atlas of mechanical properties of human cortical and cancellous bone. In: Van der Perre G, Lowet G,

Borgwardt A, editors. In vivo assessment of bone quality by vibration and wave propagation techniques. Part II. ACCO Publishing Leuven; 1991. p. 7–32.

[45] Sontag W. Quantitative measurements of periosteal and cortical-endosteal bone formation and resorption in the midshaft of female rat femur. Bone 1986;7(1):63–70.

[46] Laval-Jeantet AM, Bergot C, Carroll R, Garcia-Schaeffer F. Cortical bone senescence and mineral bone density of the humerus. Calcif Tissue Int 1983;35:268–72.

[47] R. Legros, Apport de la physico-chimie à l'étude de la phase minérale des tissus calcifiés, Master's thesis, INP Toulouse; 1978.

[48] Pellegrino E, Blitz R. Mineralization in the chick's embryo I. monohydrogen phosphate and carbonate relationship during maturation of the bone crystal complex. Calcif Tissue Int 1972;10:128–35.

[49] Magne D, Pilet P, Weiss P, Daculsi G. Fourier transform infrared microspectroscopic investigation of the maturation of nonstochiometric apatites in mineralized tissues: a horse dentin study. Bone 2001;29(6):547–52.

[50] Magne D, Weiss P, Bouler J, Laboux O, Daculsi G. Study of the maturation of the organic (type i collagen) and mineral (nonstoichiometric apatite) constituents of a calcified tissue (dentin) as a function of location: a Fourier Transform InfraRed microspectroscopic investigation. J Bone Miner Res 2001;16(4):750–7.